ISSN 1330-3651 (Print), ISSN 1848-6339 (Online)
UDC/UDK 624.044:624.166.8

ELASTIC-PLASTIC ANALYTICAL SOLUTIONS OF DEFORMATION OF UPLIFT BELLED PILE

W. J. Yao, S. P. Chen

Original scientific paper
In this paper, based on the overlapping deformation mode of load transfer law of uplift belled pile, and the theory of elastic mechanics, the elastic-plastic analytical solutions of uplift belled pile were derived, and the nonlinear elastic-plastic deformation analysis method was established, which made the deformation analysis theory of uplift belled pile more reasonable. The deformation analysis method of uplift belled pile was extended to uplift pile with change location expanding body (CLEB), which was carried out the deformation analysis of uplift pile under the complex load conditions conveniently. The deformation analytical solutions derived in this paper were simpler, avoid unit division of pile and tedious numerical calculation. Through the comparison between test results and results of theoretical calculation, it was shown that the elastic-plastic analytical solutions were close to the field test results. The elastic-plastic method in this paper provided a reference for engineering design of uplift belled pile. The method established in this paper could calculate the load-deformation relationship of uplift belled pile which has high level of bearing capacity, so it has important role to reduce or partially replace the field loading test work. Finally, the method was used to analyse the main factors of uplift belled pile of affecting the deformation character of the uplift belled pile.

Keywords: *elastic-plastic deformation, nonlinear, overlapping deformation mode, uplift belled pile, uplift pile with CLEB*

Elastično-plastična analitička rješenja deformacije vertikalnog zvonastog pilona

Izvorni znanstveni članak
U ovom radu, zasnovanom na metodi preklapajuće deformacije zakona o prijenosu opterećenja vertikalnog zvonastog pilona i na teoriji elastične mehanike, izvedena su elastično-plastična analitička rješenja vertikalnog zvonastog pilona, te je postavljena metoda analize nelinearne elastično-plastične deformacije, koja je učinila prihvatljivijom teoriju analize deformacije vertikalnog zvonastog pilona. Metoda analize deformacije vertikalnog zvonastog pilona proširena je na vertikalni pilon s ekspandirajućim tijelom promjenljive lokacije (CLEB - change location expanding body), za odgovarajuću analizu deformacije vertikalnog pilona pri složenim uvjetima opterećenja. Analitička rješenja deformacije izvedena u ovom radu jednostavnija su, izbjegavaju jediničnu podjelu pilona i zamorne numeričke proračune. Usporedbom rezultata ispitivanja i rezultata teorijskih proračuna, pokazano je da su elastično-plastična analitička rješenja bila blizu rezultata dobivenih ispitivanjima na terenu. Elastično-plastična metoda korištena u ovom radu osigurala je reference za tehnički projekt vertikalnog zvonastog pilona. Metodom postavljenom u ovom radu može se izračunati odnos opterećenje-deformacija vertikalnog zvonastog pilona koji ima visoki stupanj nosivosti, te ima važnu ulogu u smanjenju ili djelomičnoj zamjeni za ispitivanja na terenu. Konačno, ta je metoda primijenjena u analizi glavnih čimbenika vertikalnog zvonastog pilona koji djeluju na karakter deformacije vertikalnog zvonastog pilona.

Ključne riječi*: vertikalni zvonasti pilon, vertikalni pilon s CLEB, elastično-plastična deformacija, nelinearan, model preklapajuće deformacije*

1 Introduction

At present, the current theoretical design and calculation method of the uplift pile at home and abroad, in particular the uplift belled pile, is in the starting stage, the research on the uplift belled pile is mainly centralized on the bearing capacity of the uplift pile, and the research on the deformation character of the uplift pile is very rare. In the actual application process, the bearing capacity of the uplift pile is large relatively, and the bearing capacity of the pile has been controlled by deformation.

Many scholars research the nonlinear elastic-plastic deformation of uplift pile with uniform cross section and establish a nonlinear deformation analysis method [1 ÷ 4] of uplift pile with uniform cross section, but actually, the deformation calculation of the uplift belled pile is more complex than the deformation of the uplift pile with uniform cross section. To calculate the deformation of uplift belled pile accurately, there are some difficulties [5] in theory and in practice. This paper is aimed to researching the nonlinear elastic-plastic deformation of uplift belled pile and establishing a nonlinear deformation analysis method of uplift belled pile. When the uplift load on the top of the uplift belled pile is small, the soil on the side of the pile is in the elastic state, and relative slippage occurs between the pile and the soil, the deformation character of the uplift belled pile can be analysed accurately based on the elastic deformation analysis method of the soil on the side of the pile at this moment. However, when the uplift load on the top of the pile is large, the soil on the side of the pile is transited from the elastic state to the plastic state and the plastic zone is extended from the top of the pile to the pile tip, a certain error will be generated by performing elastic theoretical analysis for the deformation of the uplift belled pile at this moment. In this paper, based on the overlapping deformation mode of load transfer law of uplift belled pile, and the theory of elastic mechanics, the elastic-plastic analytical solutions of uplift belled pile are derived, and the nonlinear elastic-plastic deformation analysis method is established, which makes the deformation analysis theory of uplift belled pile more reasonable. The deformation analysis method of uplift belled pile is extended to uplift pile with CLEB, which carried out the deformation analysis of uplift pile under the complex load conditions conveniently.

2 Analysis model of uplift belled pile

The theoretical analytical solutions of uplift load and displacement of belled pile is derived by considering the sliding character between the pile and the soil based on the elastic deformation analysis [6] of uplift pile with uniform cross section.

The analysis diagrammatic sketch of uplift belled pile is shown in Fig. 1 as follows.

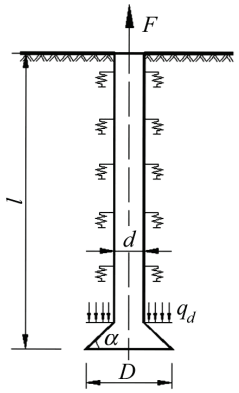

Figure 1 Analysis diagrammatic sketch of uplift belled pile

Under the working load effect, the displacement on the expanding body of the uplift belled pile is small generally. However, the situation is not reported in the literature of the research on the nonlinear relationship between the pile-tip counter force and the displacement of the uplift belled pile at home and abroad. Thus, in order to simplify the analysis, it is assumed that the elastic relationship between the pile-tip counter force and the displacement is reasonable. Fig. 1 can be simplified to Fig. 2.

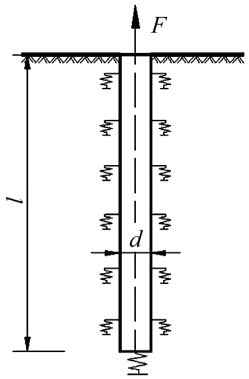

Figure 2 Load transfer analysis model of uplift belled pile

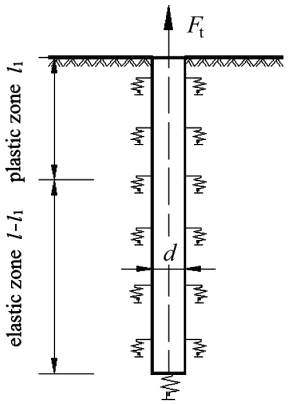

Figure 3 Displacement analysis model of uplift belled pile

When the uplift load on the top of the uplift pile is large, the pile-soil system is in the elastic stage mainly, and relative slippage does not occur between the pile and the soil. When the uplift load is increased gradually, the soil on the side of the pile is transited from the elastic state to the plastic state gradually, relative slippage occurs between the pile and the soil, and the plastic zone is extended from the top of the pile to the pile tip gradually. The influence of the plastic deformation for the deformation of the uplift pile shall be considered, and the displacement analysis model is shown in Fig. 3.

In order to facilitate the analytical analysis, the parameter sliding degree ψ is introduced. The plastic zone of the soil generally begins from the ground surface, and may be developed to a certain depth under a certain load level, which is called the sliding degree, and the expression is as follows:

$$0 \le \psi \le 1, \psi = \frac{l_1}{l}. \tag{1}$$

According to the definition, the pile can be divided into upper and lower segments, wherein the pile segment between the top of the pile and the depth of l_1 is the plastic zone, and the pile segment between the depth of $l - l_1$ is the elastic zone.

In order to analyze the elastic-plastic deformation of the uplift belled pile, it is assumed as follows:

1) The uplift pile is kept in the elastic state in the uplift load process. That is, the influence of the pile tension plastic deformation on the elastic modulus of the pile is not considered;
2) The $\tau - z$ curve of the soil on the side of the pile is a perfect elastic-plastic model, and the limit friction resistance of the soil on the side of the pile will be changed in power function along with the depth;
3) The shear modulus of the soil on the side of the pile is a constant.

For the second assumption, Guo, Randolph and the like think that the limit friction resistance of the soil and the depth are changed in power function [7 ÷ 10], i.e.:

$$\tau_f(z) = kz^{\alpha}, \tag{2}$$

in the formula: k and α are the parameters of power function.

The third assumption, that the shear modulus of the soil on the side of the pile is a constant, is reasonable for the homogeneous soil. For the normal consolidation soil, the shear modulus of the soil is generally increased linearly with the depth. Motto[11] calculated and obtained the deformation value on the top of the pile according to the mean value of the modulus of the soil on the side of the pile, which was close to the deformation value on the top of the pile calculated and obtained by the linear increase of the soil modulus. This shows that the third assumption is reasonable.

3 Elastic-plastic deformation analysis

3.1 Plastic pile segment l_1

Within the depth l_1, the friction resistance of the soil reaches the limit friction resistance $\tau_f(z)$ completely. At the depth l_1 and below, the soil is still in the elastic state, the pile segment with the depth of l_1 and above is the plastic zone. The deformation of the pile body at the depth of l_1 is δ_A, and the axial force of the pile is F_A which can be interpreted as the pile-tip load for

generating the elastic deformation δ_A on the uplift pile at the pile segment with the length of $(l - l_1)$. The axial force and the displacement on the plastic segment of the pile at any depth z are as follows:

$$F(z) = F_A + \int_z^{l_1} 2\pi r_0 (kz^\alpha) \mathrm{d}z = F_A + 2\pi r_0 \frac{k(l_1^{\alpha+1} - z^{\alpha+1})}{\alpha+1}, \quad (3)$$

$$\delta(z) = \delta_A + \int_z^{l_1} \frac{F(z)}{E_p A_p} \mathrm{d}z = \delta_A + \frac{F_A(l_1 - z)}{E_p A_p} + \frac{2k\pi r_0 \left[z^{\alpha+2} + (\alpha+1)l_1^{\alpha+2} - (\alpha+2)l_1^{\alpha+1} z\right]}{E_p A_p (\alpha+1)(\alpha+2)}, \quad (4)$$

in which, r_0 is the radius of the pile.

The displacement and the axial force on the top of the pile can be obtained from Eq. (3) and Eq. (4):

$$\delta_t = \delta(z)\big|_{z=0} = \delta_A + \frac{F_A l_1}{E_p A_p} + \frac{2k\pi r_0 l_1^{\alpha+2}}{E_p A_p (\alpha+2)}, \quad (5)$$

$$F_t = F(z)\big|_{z=0} = F_A + \frac{2k\pi r_0 l_1^{\alpha+1}}{\alpha+1}. \quad (6)$$

3.2 Elastic pile segment $(l - l_1)$

The uplift pile is the pile with the limited stiffness, the control differential equation of single pile based on overlapping deformation mode is as follows:

$$\frac{\partial^2 \delta(z)}{\partial^2 z} = \frac{2\tau_0(z)}{r_0^2 \xi \lambda}, \quad (7)$$

in which, $\xi = \ln\left(\frac{r_m}{r_0}\right)$ and $\lambda = \frac{E_p}{G_s}$.

The solution expression of the equation above is as follows:

$$\delta(z) = c_1 e^{\mu z} + c_2 e^{-\mu z}, \quad (8)$$

in which, $\mu = \left(\frac{2}{r_0^2 \lambda \xi}\right)^{0,5}$.

For Eq. (8), the boundary condition is as follows:

$$\delta_b = \delta(z)\big|_{z=l} = \frac{F_b(1-\nu_s)}{4 r_0 G_s}\eta, \quad (9)$$

$$\left.\frac{\mathrm{d}\delta(z)}{\mathrm{d}z}\right|_{z=l} = \frac{-F_b}{\pi r_0^2 \lambda G_s}, \quad (10)$$

in which, $\eta = \frac{r_0}{r_0 + r_b}$, and Eq. (9) is derived in the references [12] in this paper.

The obtained coefficients c_1 and c_2 are substituted into Eq. (8) to give:

$$\delta(z) = \frac{F_b}{2 r_0 G_s}\left\{\left[\frac{1}{\pi r_0 \lambda \mu} + \frac{(1-\nu_s)\eta}{4}\right] e^{\mu(l-z)} + \left[\frac{1}{\pi r_0 \lambda \mu} + \frac{(1-\nu_s)\eta}{4}\right] e^{-\mu(l-z)}\right\} = \frac{F_b}{r_0 G_s}\left\{\frac{(1-\nu_s)\eta}{4}\mathrm{ch}[\mu(l-z)] + \frac{1}{\pi r_0 \lambda \mu}\mathrm{sh}[\mu(l-z)]\right\}. \quad (11)$$

The axial force on the plastic segment of the pile at any depth z is as follows:

$$F(z) = F_b \pi r_0 \lambda \mu \left\{\frac{(1-\nu_s)\eta}{4}\mathrm{ch}[\mu(l-z)] + \frac{1}{\pi r_0 \lambda \mu}\mathrm{sh}[\mu(l-z)]\right\}. \quad (12)$$

Generally, the uplift pile used in the project shall be designed by controlling the tension crack within 0,2 mm [13], the elastic modulus of the pile is usually high, and $1/(\pi r_0 \lambda \mu)$ in the Eq. (12) is very small, so $\delta(z)$ can be simplified as follows:

$$\delta(z) = \frac{F_b}{r_0 G_s}\frac{(1-\nu_s)\eta}{4}\mathrm{ch}[\mu(l-z)] \approx w_b \mathrm{ch}[\mu(l-z)]. \quad (13)$$

In case of $z = l_1$, the deformation δ_A and the axial force F_A at the bottom of the plastic pile segment ($z = l_1$) are respectively as follows:

$$\delta_A = \delta(z)\big|_{z=l_1} = \frac{F_b}{r_0 G_s}\left\{\frac{(1-\nu_s)\eta}{4}\mathrm{ch}[\mu(l-l_1)] + \frac{1}{\pi r_0 \lambda \mu}\mathrm{sh}[\mu(l-l_1)]\right\}, \quad (14)$$

$$F_A = F(z)\big|_{z=l_1} = F_b \pi r_0 \lambda \mu \left\{\frac{(1-\nu_s)\eta}{4}\mathrm{sh}[\mu(l-l_1)] + \frac{1}{\pi r_0 \lambda \mu}\mathrm{ch}[\mu(l-l_1)]\right\}. \quad (15)$$

Through the analysis above, the dimensionless expression on the elastic pile segment $(l - l_1)$ of the uplift belled pile can be obtained based on Eq. (14) and Eq. (15):

$$\frac{F_A}{r_0 G_s \delta_A} = \frac{\pi r_0 \lambda \mu \rho\, \mathrm{sh}[\mu(l-l_1)] + \mathrm{ch}[\mu(l-l_1)]}{\rho\, \mathrm{ch}[\mu(l-l_1)] + \frac{1}{\pi r_0 \lambda \mu}\mathrm{sh}[\mu(l-l_1)]}, \quad (16)$$

in which, $\rho = \frac{(1-\nu_s)\mu}{4}$.

According to the Eqs. (2) and (16), the following expressions are derived:

$$\delta_A = \xi \frac{\tau_f(z) r_0}{G_s} = \xi \frac{k z^\alpha r_0}{G_s}, \quad (17)$$

$$F_{\mathrm{A}}=\delta_{\mathrm{A}} r_0 G_{\mathrm{s}} \frac{\pi r_0 \lambda\mu\rho\,\mathrm{sh}\left[\mu(l-l_1)\right]+\mathrm{ch}\left[\mu(l-l_1)\right]}{\rho\,\mathrm{ch}\left[\mu(l-l_1)\right]+\dfrac{1}{\pi r_0\lambda\mu}\mathrm{sh}\left[\mu(l-l_1)\right]}. \quad (18)$$

The axial force and the displacement on the top of the uplift belled pile can be obtained by integrating two pile segments in collection with the formula (5) and the formula (6):

$$\delta_{\mathrm{t}}=\delta_{\mathrm{A}}\left\{1+\frac{r_0 G_{\mathrm{s}} l_1}{E_{\mathrm{p}} A_{\mathrm{p}}}\frac{\pi r_0\lambda\mu\rho\,\mathrm{sh}\left[\mu(l-l_1)\right]+\mathrm{ch}\left[\mu(l-l_1)\right]}{\rho\,\mathrm{ch}\left[\mu(l-l_1)\right]+\dfrac{1}{\pi r_0\lambda\mu}\mathrm{sh}\left[\mu(l-l_1)\right]}\right\}+ \quad (19)$$

$$+\frac{2k\pi r_0 l_1^{\alpha+2}}{E_{\mathrm{p}} A_{\mathrm{p}}(\alpha+2)},$$

$$F_{\mathrm{t}}=\delta_{\mathrm{A}} r_0 G_{\mathrm{s}} \frac{\pi r_0 \lambda\mu\rho\,\mathrm{sh}\left[\mu(l-l_1)\right]+\mathrm{ch}\left[\mu(l-l_1)\right]}{\rho\,\mathrm{ch}\left[\mu(l-l_1)\right]+\dfrac{1}{\pi r_0\lambda\mu}\mathrm{sh}\left[\mu(l-l_1)\right]}+\frac{2k\pi r_0 l_1^{\alpha+1}}{\alpha+1}. \quad (20)$$

3.3 Calculation method of elastic-plastic deformation

(1) For any appointed sliding degree ψ, the displacement δ_{t} and the axial force F_{t} on the top of the pile can be obtained based on the formula (19) and the formula (20). If a series of sliding degree ψ is given, the complete load-displacement relationship curve of uplift belled pile can be obtained.

(2) For the given load F_{t}, the sliding degree ψ of the uplift pile can be obtained based on the formula (20). As the equation is a nonlinear equation, the solution of equation can be obtained by the dichotomy [14], and then the sliding degree ψ shall be put into the formula (19) to obtain the displacement $w(t)$ on the top of the pile.

(3) In the previous contents, the load-displacement relationship of uplift pile under the perfect elastic-plastic condition is not only derived, but also the relationship between the axial force $F(z)$ and the displacement $\delta(z)$ of the pile under the various loads can be obtained based on the formula (3) and the formula (4).

4 Promotion of uplift belled pile: analytical solutions of uplift pile with CLEB

The main work above is to derive the elastic-plastic analytical solutions of the uplift belled pile, that is the expanding body is located on the bottom of the uplift pile. The uplift belled pile in the project is widely used. The bearing capacity of single pile can be greatly improved, and the displacement can be reduced by the uplift resistance of the expanding body while bearing the uplift load. In the actual project, the maximum allowable displacement of the uplift pile with CLEB is often taken as the important design index. How to get the load-displacement relationship of the uplift pile with expanding body is a problem to be solved urgently. This section is mainly aimed at promoting the analytical method of the uplift belled pile to the uplift pile with CLEB.

4.1 Analysis model

For the uplift pile having an expanding body on the pile, the overlapping deformation model of uplift pile with CLEB is shown in Fig. 4, and the soil deformation around the uplift pile is shown in Fig. 5.

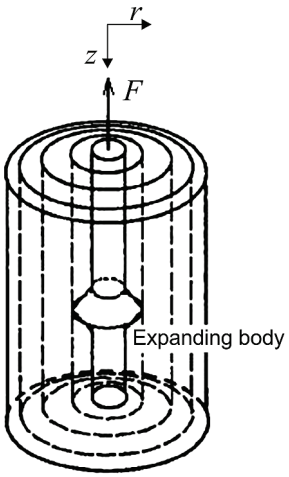

Figure 4 Overlapping deformation model of uplift pile with CLEB

There are few researches on the uplift pile with CLEB, and they are limited in the aspect of the bearing capacity mainly. In the project practice, the bearing capacity of the uplift pile is not merely taken as the design standard. The allowable deformation of the pile foundation is often strictly required. When the uplift pile with CLEB is in the working load scope of the uplift resistance, the deformation of the pile foundation is often centralized on the upper pile segment of the expanding body, in particular, in the existing uplift pile foundation design, the pile crack control calculation [15, 16] shall be performed. In the design process of the uplift pile with CLEB, the crack control calculation showed that the pile-tip deformation control value corresponds to the limit bearing capacity standard value (two times of the working load) of the pile, and the pile crack is mainly centralized on the upper pile segment of the expanding body. In the static load test process of the pile, the upper soil of the expanding body is deformed obviously, the pile crack on the lower segment of the expanding body is small and the pile-soil deformation complies with the overlapping deformation mode of Randolph&Wroth [17], it is thought that displacement coordination between the pile and the soil shall be performed. The load transfer analysis model of uplift pile with CLEB is shown in Fig. 6.

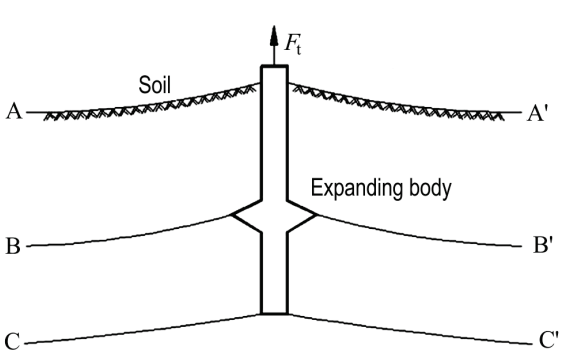

Figure 5 Soil deformation around the uplift pile with CLEB

4.2 Expanding body

The expanding body shall be projected on the horizontal plane and can be simplified to be a rigid circular ring pressing plate acting on the semi-infinite elastic foundation. When the pile bears the uplift load, the upper soil is also extruded by the rigid circular ring. The upward displacement of the soil at the expanding body is derived as follows:

$$\delta_{\mathrm{C}}=\frac{\pi(1-\nu_{\mathrm{s}}^2)\left(\frac{D}{2}-r_0\right)}{2E_{\mathrm{sb}}}\cdot\frac{F_{l_2}}{\pi\left[\left(\frac{D}{2}\right)^2-r_0^2\right]}=\\ =\frac{F_{l_2}(1-\nu_{\mathrm{s}})}{4G_{\mathrm{sb}}\left(\frac{D}{2}-r_0\right)}. \tag{21}$$

in which, E_{sb} and G_{sb} are the modulus of deformation and the shear modulus of the soil at the expanding body, respectively, and $E_{\mathrm{sb}}=2G_{\mathrm{sb}}(1+\nu_{\mathrm{s}})$.

The formula above shall be simplified:

$$F_{l_2}=K_1\delta_{\mathrm{C}}, \tag{22}$$

in which, K_1 is the stiffness coefficient of the expanding body, $K_1=4G_{\mathrm{sb}}\frac{\frac{D}{2}+r_0}{1-\nu_{\mathrm{s}}}$, and δ_{C} is the bottom cross-section displacement of the pile segment on the upper part of the expanding body.

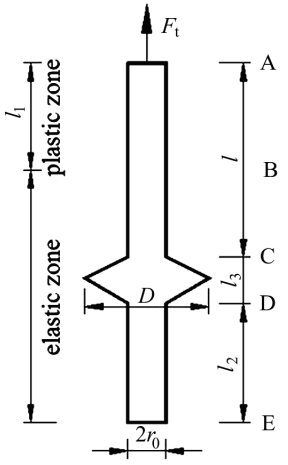

Figure 6 Load transfer analysis model of uplift expanding pile

As shown in Fig. 6 above:

$$F_{\mathrm{t}}=F_l+F_{l_2}+F_{l_3}, \tag{23}$$

in which, F_l is the lateral friction resistance of the upper pile segment of the expanding body, F_{l_2} is the uplift resistance of the expanding body, and F_{l_3} is the lateral friction resistance of the lower pile segment of the expanding body.

4.3 Lower pile segment of expanding body

For the lower pile segment of the expanding body, the differential equation of the pile displacement is as follows:

$$\frac{\partial^2\delta(z)}{\partial z^2}=\frac{2\partial\delta(z)}{\lambda\xi r_0^2}, \tag{24}$$

in which, $\lambda=\frac{E_{\mathrm{p}}}{G_{\mathrm{p}}}$ and the general solution of the equation is as follows: $\delta(z)=c_1\mathrm{e}^{\mu z}+c_2\mathrm{e}^{-\mu z}$, wherein $\mu=\left(\frac{2}{\lambda\xi r_0^2}\right)^{0,5}$, c_1 and c_2 are undetermined constants. The boundary conditions of the differential equation are as follows:

$$\left.\frac{\partial\delta(z)}{\partial z}\right|_{z=l+l_2}=-\frac{F_{l_3}}{\pi r_0^2\lambda G_{\mathrm{s}}},\ \text{i.e. } \mu(c_1-c_2)=-\frac{F_{l_3}}{\pi r_0^2\lambda G_{\mathrm{s}}}, \tag{25}$$

$$\left.\frac{\partial\delta(z)}{\partial z}\right|_{z=l+l_2+l_3}=0,\ \text{i.e. } \mu(c_1\mathrm{e}^{\mu l_3}-c_2\mathrm{e}^{-\mu l_3})=0. \tag{26}$$

The analytical expression of the lower pile segment is as follows:

$$F_{l_3}=K_2\delta_{\mathrm{D}}, \tag{27}$$

inwhich, K_2 is the stiffness coefficient of the lower pile segment of the expanding body, $K_2=\pi r_0^2\mu_1\lambda G_s\ \mathrm{th}(\mu_1 l')\delta_{\mathrm{C}}$, wherein $\mu_1=\left(\frac{2}{\lambda\xi_1 r_0^2}\right)^{0,5}$, $\xi_1=\ln\left(\frac{2{,}5l'(1-\nu_{\mathrm{s}})}{r_0}\right)$, considering the size effect [17] of the expanding body, the calculation length of the lower pile segment of the expanding body is $l'=l_3+\frac{Dl_2}{4r_0}$, and δ_{D} is the top cross-section displacement of the lower pile segment of the expanding body (i.e. the displacement on the lower end of the expanding body).

4.4 Upper pile segment of expanding body

For the elastic zone of the upper pile segment of the expanding body, the differential Eq. (24) of the pile displacement is also established, but the boundary conditions are different from those of the lower pile segment of the expanding body. The axial force of the lower end is as follows:

$$F_{\mathrm{C}}=F_{l_2}+F_{l_3}. \tag{28}$$

The uplift load on the top cross-section of the elastic zone on the upper pile segment of the expanding body is as follows:

$$F_{\mathrm{B}} = F_{\mathrm{C}} + F_{l-l_1}. \tag{29}$$

The inherent extension deformation of the expanding body is ignored herein, the upper and lower ends of the expanding body have the same displacement, i.e.:

$$\delta(z)\big|_{z=l} = \delta(z)\big|_{z=l+l_2},\ \text{i.e.}\ \delta_{\mathrm{C}} = \delta_{\mathrm{D}}. \tag{30}$$

The axial force on the lower end of the upper pile segment is as follows:

$$F_{\mathrm{C}} = F(z)\big|_{z=l} = F_{l_2} + F_{l_3} = K_1\delta_{\mathrm{C}} + K_2\delta_{\mathrm{D}} = (K_1 + K_2)\delta_{\mathrm{C}}, \tag{31}$$

Consider that the boundary conditions are located at the lower end of the upper pile segment:

$$\delta_{\mathrm{B}} = \delta(z)\big|_{z=l} = \frac{F_{\mathrm{C}}}{K_1 + K_2}, \tag{32}$$

$$\left.\frac{\partial\delta(z)}{\partial \mathrm{z}}\right|_{z=l} = -\frac{F_{\mathrm{C}}}{\pi r_0^2 \lambda G_{\mathrm{s}}}. \tag{33}$$

The general expression of displacement, i.e. $\delta(z) = c_1 \mathrm{e}^{\mu z} + c_2 \mathrm{e}^{-\mu z}$ shall be put in the boundary conditions, it is assumed that $z = l_1$, the displacement on the top of the pile is as follows:

$$\delta_{\mathrm{B}} = \delta(z)\big|_{z=l_1} = F_{\mathrm{C}}\left\{\frac{1}{K_1 + K_2}\mathrm{ch}\left[\mu(l-l_1)\right] + \right.$$
$$\left. + \frac{1}{\pi r_0^2 \lambda G_{\mathrm{s}} \mu}\mathrm{sh}\left[\mu(l-l_1)\right]\right\}, \tag{34}$$

in which, $\mu = \left(\frac{2}{\lambda\xi r_0^2}\right)^{0,5}$, and $\xi = \ln\left(\frac{2{,}5l(1-\nu_{\mathrm{s}})}{r_0}\right)$.

According to the elastic compression condition and $z = 0$, the uplift load on the top cross-section in the elastic zone of the upper pile segment of the expanding body is as follows:

$$F_{\mathrm{B}} = F_{\mathrm{C}}\left\{\frac{\pi r_0^2 \lambda G_{\mathrm{s}} \mu}{K_1 + K_2}\mathrm{sh}\left[\mu(l-l_1)\right] + \mathrm{ch}\left[\mu(l-l_1)\right]\right\}. \tag{35}$$

The dimensionless expression on the uplift load and the displacement of the top cross-section, i.e. the cross-section B in the elastic zone on the upper pile segment of the expanding body can be obtained based on Eq. (34) and Eq. (35):

$$\frac{F_{\mathrm{B}}}{G_{\mathrm{s}} r_0 \delta_B} = \pi r_0 \lambda\mu \frac{1 + \eta_1 \tan\left[\mu(l-l_1)\right]}{\eta_1 \tan\left[\mu(l-l_1)\right]}. \tag{36}$$

In which,

$$\eta_1 = \frac{\pi r_0^2 \lambda G_{\mathrm{s}} \mu}{K_1 + K_2} = \frac{\pi r_0^2 \lambda G_{\mathrm{s}} \mu}{\frac{4\left(\frac{D}{2} + r_0\right)G_{\mathrm{sb}}}{1-\nu_{\mathrm{s}}} + \pi r_0^2 \lambda G_{\mathrm{s}} \mu \tan(\mu_1 l')}.$$

The axial force and the displacement of the plastic segment at any depth z of the pile can be represented as follows:

$$F(z) = F_{\mathrm{B}} + \int_z^{l_1} 2\pi r_0 (kz^{\alpha})\mathrm{d}z = F_{\mathrm{B}} + 2\pi r_0 \frac{k(l_1^{\alpha+1} - z^{\alpha+1})}{\alpha+1}, \tag{37}$$

$$\delta(z) = \delta_{\mathrm{B}} + \int_z^{l_1} \frac{F(z)}{E_{\mathrm{p}} A_{\mathrm{p}}}\mathrm{d}z = \delta_{\mathrm{B}} + \frac{F_{\mathrm{B}}(l_1 - z)}{E_{\mathrm{p}} A_{\mathrm{p}}} +$$
$$+ \frac{2k\pi r_0\left[z^{\alpha+2} + (\alpha+1)l_1^{\alpha+2} - (\alpha+2)l_1^{\alpha+1} z\right]}{E_{\mathrm{p}} A_{\mathrm{p}} (\alpha+1)(\alpha+2)}. \tag{38}$$

The axial force and the displacement on the top of uplift pile with CLEB can be obtained as follows:

$$\frac{F_{\mathrm{B}}}{G_{\mathrm{s}} r_0 \delta_B} = \pi r_0 \lambda\mu \frac{1 + \eta_1 \tan\left[\mu(l-l_1)\right]}{\eta_1 \tan\left[\mu(l-l_1)\right]}.$$

$$\delta_{\mathrm{t}} = \delta_{\mathrm{B}}\left\{1 + \frac{r_0 G_{\mathrm{s}} l_1}{E_{\mathrm{p}} A_{\mathrm{p}}} \frac{\pi r_0 \lambda\mu\rho\ \mathrm{th}\left[\mu(l-l_1)\right] + 1}{\rho + \frac{1}{\pi r_0 \lambda\mu}\mathrm{th}\left[\mu(l-l_1)\right]}\right\} + \tag{39}$$
$$+ \frac{2k\pi r_0 l_1^{\alpha+2}}{E_{\mathrm{p}} A_{\mathrm{p}} (\alpha+2)},$$

$$F_{\mathrm{t}} = \delta_{\mathrm{B}} G_{\mathrm{s}} A_{\mathrm{p}} \lambda\mu \frac{1 + \eta_1 \tan\left[\mu(l-l_1)\right]}{\eta_1 + \tan\left[\mu(l-l_1)\right]} + \frac{2k\pi r_0 l_1^{\alpha+1}}{\alpha+1}. \tag{40}$$

For the uplift pile with CLEB of the actual project, the expanding body is often buried on the bottom of the uplift pile, the lower pile segment below the expanding body does not exist, i.e. $l_2 = 0$. At this moment, the uplift belled pile is the special example of the uplift pile with CLEB.

5 Project examples

Example 1: Single building type single layer underground garage of Shanghai Ruijin Hospital is featured with the buried depth of the garage foundation of 5,8 m, the plane size of about 40 × 90 m and the total area of about 3500 m^2. The soil of about 1m thickness covers the top plate and to be the greening and fitness leisure place. The soil distribution and main physical mechanical comprehensive index in the scope of 40m depth below the earth's surface is shown in Tab. 1. The underground water on the shallow part of the foundation belongs to the type of phreatic water. Main supply source is the atmospheric precipitation. The water level will be changed along with the season. The buried depth of the stable water level is 0,8 to 1,0 m.

The garage shall meet the requirements of the double layer mechanical garage. In the design, a series of measures have been taken to reduce the floor height of the garage as much as possible, but the garage still bears high buoyancy, and cannot meet the anti-floating requirements with the self-weight of the structure only. In case of the ordinary uplift pile of uniform section, the cast-in-situ bored pile of uniform section with the pile diameter of 600 mm can be used according to the geological conditions of the site. The effective pile length is 22 m (the buried depth is about 29 m), the depth of entering into the gray loam layer is about 3,5 m, and there are 256 piles totally. In order to improve the economical efficiency of the uplift pile, the above-mentioned cast-in-situ bored pile of uniform section shall be replaced by the uplift belled pile. The size of the enlarged bottom is shown in Fig. 7. The pile diameter in the uniform section part of the uplift belled pile is 400 mm, the maximum diameter of the uplift belled pile is 800 mm, the height of the enlarged bottom is about 1,5 m, and the total pile length is not changed. According to the inverse analysis of the geological exploration data, the increase in the limit friction resistance of the soil on the side of the pile is k = 2,13 kPa, and the index of the power function is α = 0,9.

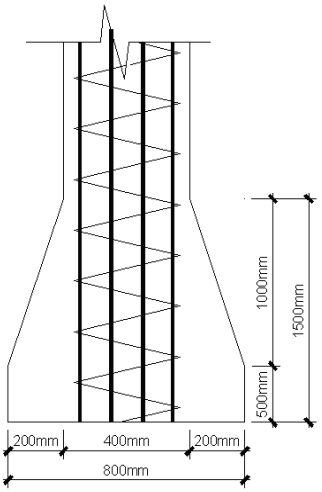

Figure 7 Size of enlarged bottom of uplift belled pile

The static uplift load test is performed for multiple groups of single pile in the project. Due to the similarity of the site condition, the measured load-displacement relationship curve of uplift belled pile 88# is selected to compare with the theoretical calculation curve herein.

Table 1 The soil distribution and main physical mechanical index

Soil layer No.	Soil layer name	Thickness	Density	Void ratio	Modulus of compression	Internal friction angle	Cohesion
		m	kg/m^3	e	$E_{s1\text{-}2}$ / MPa	φ / °	c / kPa
1	Brown yellow clay	2	1880	0,954	3,59	14,5	15
2	Gray silt loam	3	1780	1,184	2,84	21	6
3	Gray silt clay	10	1730	1,373	1,83	8,5	9
4	Gray clay	7	1800	1,104	3,23	8,5	10
5	Gray loam	22	1810	0,985	4,07	18	13
6	Grey sand loam	1	1920	0,739	8,39	25	6
7	Grey green silt	3	1960	0,724	14,13	28,5	3
8	Dark green loam	12	2100	0,530	8,34	28	41

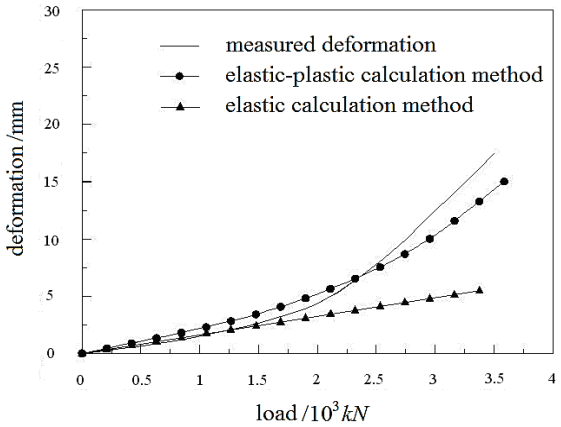

Figure 8 The comparison between measured value and theoretical value of uplift belled pile 88# (pile length=51 m)

As shown in Fig. 8, the theoretical result obtained by the elastic-plastic calculation method is basically close to the measured value in the paper; this shows that the nonlinear deformation of the uplift belled pile can be calculated well by the elastic-plastic calculation method in the paper. Fig. 8 also shows that theoretical load-displacement curve obtained by the elastic-plastic calculation method is close to the measured curve. When the load on the top of the pile is large, the theoretical deformation result is greatly different from the measured deformation value of the pile, and the elastic calculation method of the uplift belled pile only can be used for calculating the deformation of the uplift belled pile in the low load level accurately.

Example 2: Shanghai South Railway Station is a landmark project constructed for solving the shortage of the existing passenger transport hub capacity in Shanghai, the overall is designed by East China Architectural Design Institute, wherein the south square, designed by Shanghai Municipal Design Institute, is mainly composed of underground garage, market, sunken plaza and various underground passages. The underground garage and the market are the underground two-layer structures, the underground passages are underground one-layer structure, and the sunken plaza is the connection area between the underground garage and the south hall outbound of the main station.

The project belongs to the typical deep foundation, and the maximum excavation depth of the foundation pit shall be in line with 14,0 m. The load type mainly includes anti-floating and anti-foundation uplift types. The uplift belled pile foundation [18] is used in the design as shown in Fig. 9. The south square project, located in the center of South Station in Shanghai, has the groundwater depth of 0,5 m throughout the year and belongs to the strand plain

geomorphic type. In the design, the expanded-base cast-in-situ bored pile is taken as the uplift foundation. The expanded-base method uses the mechanical extrusion and expansion, wherein the length of test pile A is 44 m, the pile diameter is 600 mm, the expanded-base diameter is 1150 mm, and the expanded-base part is 1 m high. The length of test pile B is 51 m, and the expanded-base diameter and height are the same as those of pile A. The enlarged bottom is buried on the sand soil layer to obtain large uplift tension. The physical mechanical index of various soil layers in test site is shown in Tab. 2.

Table 2 The physical mechanical index of various soil layers in project site

Soil layer No.	Soil layer name	Average thickness / m	Physical mechanical index of soil layer						
			w / %	γ / kN/m^3	c / kPa	φ / °	$a_{0,1\text{-}0,2}$ / MPa^{-1}	$E_{s0,1\text{-}0,2}$ / MPa	p_s / MPa^{-1}
1	Miscellaneous fill	3,4	29,4	19,1					
2	Silty clay	1,6	35,7	18,5	20,0	15,0	0,53	3,87	0,77
3	Muddy-silty clay	2,7	43,0	17,8	13,0	15,1	0,75	3,04	0,61
4	Mucky clay	16,5	51,5	17,0	10,9	11,4	1,19	2,13	0,51
5_{-1}	Mucky clay	3,2	40,2	17,9	13,0	15,3	0,67	3,32	1,02
5_{-2}	Silty clay	8,2	32,3	18,5	3,0	31,0	0,19	10,96	4,88
5_{-31}	Silty clay and silt	17,1	35,4	18,1	17,2	16,7	0,46	4,60	1,62
5_{-32}	Green silty clay	2,4	27,8	18,8	4,5	30,6	0,27	7,37	4,62
5_{-4}	Green silty clay	1,7	24,3	19,9	44,7	18,2	0,22	8,10	3,70
7_{-1}	Sandy silt	3,7	28,4	19,3	3,3	30,7	0,17	11,14	9,02
7_{-2}	Silt	Unperforated	25,8	19,8	1,8	32,0	0,10	18,08	16,73

In the example, it is assumed that the elastic modulus of the test pile is E_p = 30 GPa. In the section, the various parameters required for the deformation analysis of the uplift belled pile shall be derived by the physical mechanical index of the various soil layers of the test site. The weighted average of the soil parameters around the test pile can be obtained according to the thickness of the various soil layers in Tab. 2. The volume-weight weighted value of the soil on the side of pile A is γ=16,4 kN/m^3, the average cohesive force is c = 11,4 kPa, the average internal friction angle is φ = 17,2°, and the average modulus of compression is E_s= 4,7 MPa. The volume-weight weighted value of the soil on the side of pile B is γ = 17,8 kN/m^3, the average cohesive force is c = 12,3 kPa, the average internal friction angle is φ = 17,12°, and the average modulus of compression is E_s = 4,7 MPa. As shown in Tab. 2, both ends of the piles A and B enter into the soil layer ⑤$_{-31}$ for a certain depth, and the depth is ten times more than the pile diameter. However, the modulus of compression of the soil layer ⑤$_{-31}$ is close to the average modulus of compression of the soil layer, and the Poisson ratio of the soil layer on the top of the enlarged bottom is v_s = 0,4. The shear modulus of the soil around the pile is G_s = 11 MPa by the inverse analysis method. The shear strength of the soil is the power function index α = 0,9. The increase in the limit friction resistance of the soil on the side of the pile A is k = 2,4 kPa, and the increase in the limit friction resistance of the soil on the side of the pile B is k = 2,0 kPa. The theoretical load-displacement curve of the uplift pile under different load effects shall be obtained by the elastic-plastic analytical expression of uplift belled pile derived in this paper and obtained by the elastic method. As shown in Fig. 10 and Fig. 11, the deformation of the uplift belled pile in the low load level can only be accurately forecasted by the elastic analytical solution of uplift belled pile. When the load is large, the elastic theoretical solution is greatly different from the measured deformation value.

The elastic-plastic load-displacement curve of uplift belled piles A and B shall be obtained by giving a series of sliding coefficients ψ and performing calculations based on Eq. (19) and Eq. (20).

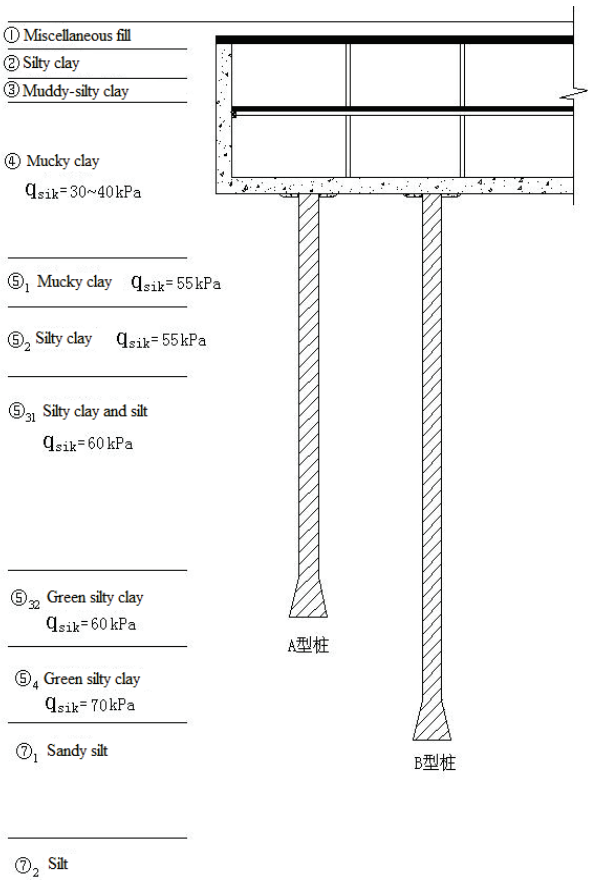

Figure 9 The sketch of uplift belled pile and soil distribution

As shown in Fig. 10 and Fig. 11, the theoretical load-displacement curve obtained by the elastic-plastic analytical expression is also close to the measured curve, and this shows that the deformation value of the uplift belled pile can be forecasted by the elastic-plastic analytical expression of uplift belled pile derived in this paper, which has a good project application prospect.

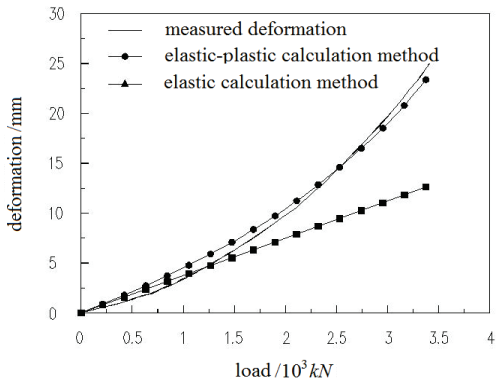

Figure 10 The comparison between measured value and theoretical value of uplift belled pile type A (pile length=44 m)

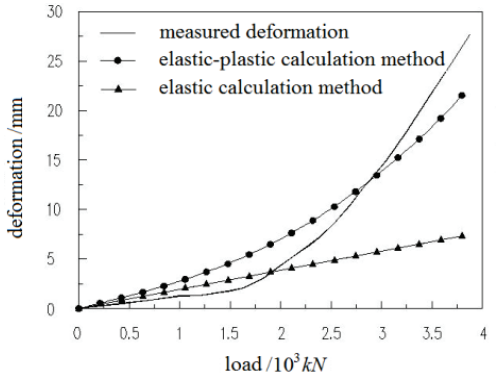

Figure 11 The comparison between measured value and theoretical value of uplift belled pile type B (pile length=51 m)

6 Parameter impact analysis

In order to research the factors of affecting the deformation character of the uplift belled pile, under the premise that the South Station in Shanghai has the same weighted average value of the soil indexes, it is assumed that the lengths of the uplift belled pile are 20 m, 30 m, 40 m and 50 m, respectively, and the diameter of the pile section of the uniform section is 1000 mm, the diameter of the enlarged bottom is 1200 mm, 1800 mm and 2400 mm, and the elastic modulus of the pile is 25 GPa, 35 GPa and 45 GPa. In order to facilitate the comparison, only one parameter shall be changed in the parameter analysis process, and other parameter shall not be changed.

(1) Pile length

The diameter of the pile segment of the uniform cross-section is 1000 mm, the diameter of the enlarged bottom is 1200 mm, and the elastic modulus of the pile is 25 GPa. Fig. 12 shows the comparison of the load-displacement curves of uplift belled pile when the pile length is different. As shown in Fig. 12, the deformation of the uplift belled pile with the length of 50 m is less than that of the pile with the length of 20 m, and the deformation of the uplift belled pile with the length of 40 m is close to that of the pile with the length of 50 m, and this shows that the pile length is inversely proportional to the deformation of the uplift belled pile, when the pile length is large, the influence of the pile length on the deformation of the belled pile is small.

Fig. 13 shows the load-displacement curves that the uplift pile of uniform section is changed with the pile length under the same parameter condition. In order to research the influence of the enlarged bottom on the deformation of the uplift pile, two figures are compared for analysis. As shown in Fig. 12 and Fig. 13, when the pile length is 20 m, the deformation of the belled pile is obviously less than that of the pile of uniform section. However, when the pile length is 50 m, the deformation of the belled pile is a little less than that of the pile of uniform section, and this shows that for the short pile, the deformation of the uplift belled pile can be reduced remarkably by the enlarged bottom. However, for the long uplift belled pile, the influence of the enlarged bottom on the deformation of the uplift belled pile is relatively small.

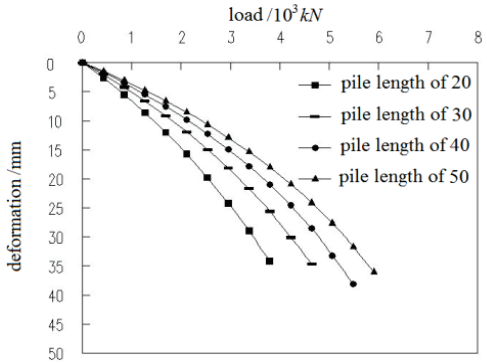

Figure 12 The relationship between load-displacement curve and pile length of uplift belled pile

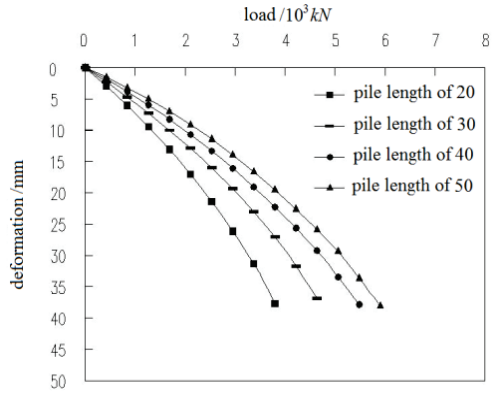

Figure 13 The relationship between load-displacement curve and pile length of uplift pile

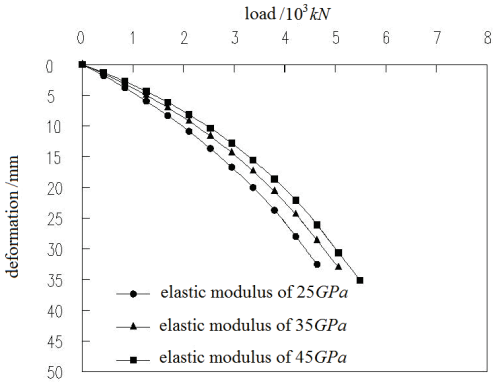

Figure 14 The relationship between load-displacement curve and elastic modulus of uplift belled pile

(2) Elastic modulus of pile

The pile length is 30 m, the diameter of the pile segment of uniform cross-section is 1000 mm, and the

diameter of the enlarged bottom is 1800 mm. Fig. 14 is the comparison of the load-displacement curves of uplift belled pile when the elastic modulus is different. As shown in Fig. 14, the influence of the elastic modulus of the pile for the deformation of the belled pile is small, and the deformation of the belled pile with the elastic modulus of 25 GPa is less than that of the belled pile with the elastic modulus of 45 GPa. However, the difference of both is small.

(3) Diameter of enlarged bottom

The pile length is 30 m, the diameter of the pile section of uniform section is 1000 mm, and the elastic modulus of the pile is 35 GPa. Fig. 15 is the comparison of the load-displacement curves of uplift belled pile when the diameter of the enlarged bottom at the end of the pile is different. As shown in Fig. 15, when the uplift load is small, the influence of the enlarged bottom at the end of the pile on the deformation of the belled pile is small, because very few loads are transferred to the end of the pile, even if there is no load transferred to the end of the pile, and the function of the expanding body at the end of the pile is not shown, e.g. when the load is less than 400 kN, there is a little uplift deformation difference among three belled piles. However, when the uplift load is large, the load has been transferred to the end of the pile, and the bearing function of the enlarged bottom has been shown gradually, the deformation of the belled pile will be reduced continuously with the increase in the diameter of the enlarged bottom. As shown in Fig. 15, when the load is more than 400 kN, the diameter of the uplift pile with the diameter of enlarged bottom at 2,4 m is obviously less than that of the uplift pile with the diameter of enlarged bottom at 1,2 m.

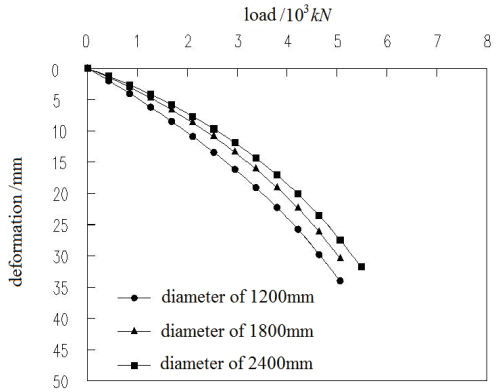

Figure 15 The relationship between load-displacement curve and expanding head diameter of uplift belled pile

7 Conclusions

1) In this paper, based on the overlapping deformation mode of load transfer law of uplift belled pile, and the theory of elastic mechanics, the elastic-plastic analytical solutions of uplift belled pile are derived, and the nonlinear elastic-plastic deformation analysis method is established, which makes the deformation analysis theory of uplift belled pile more reasonable, and the specific calculation steps are provided. At last, the deformation analysis method of uplift belled pile is extended to uplift pile with CLEB, and the deformation analysis is carried out of uplift pile under the complex load conditions conveniently.

2) The analytical deformation solutions derived in this paper are simpler, and avoid unit division of pile and tedious numerical calculation. Through the comparison between test results and results of theoretical calculation, it is shown that when the load is small, the deformation of the uplift belled pile can be calculated by the elastic deformation analysis method of the uplift belled pile well, and when the load is large, because of the nonlinear characteristics of soil, the difference between the theoretical deformation value and the measured value obtained by the elastic deformation analysis formula is large, but the elastic-plastic analytical solution is close to the field test results. The elastic-plastic method in this paper provides a reference for engineering design of uplift belled pile in the normal working state. The method established in this paper can calculate the load-deformation relationship of uplift belled pile which has high level of bearing capacity, so its role is important to reduce or partially replace the field loading test work.

3) Finally, the method is used to analyze the main factors impacting the deformation character of uplift belled pile to obtain the following conclusions:

The pile length is inversely proportional to the deformation of the uplift belled pile. When the pile length is large, the influence of the pile length on the deformation of the uplift belled pile is small. Compared with the uniform cross-section pile, for the short uplift belled pile, the deformation of the uplift belled pile can be reduced remarkably by the enlarged bottom. However, for the long uplift belled pile, the influence of the enlarged bottom on the deformation of the uplift belled pile is relatively small, and the influence of the elastic modulus of the pile on the deformation of the uplift belled pile is not obvious. When the uplift load on the top of the pile is small, the influence of the enlarged bottom at the end of the pile on the deformation of the belled pile is small. However, when the uplift load on the top of the pile is large, the load has been transferred to the end of the pile, the bearing function of the enlarged bottom has been shown gradually, and the deformation of the uplift belled pile will be reduced continuously with the increase in the horizontal size of the enlarged bottom.

8 References

[1] Vaziri, H. H.; Xie, J. Method for analysis of axially loaded piles in nonlinear soils. // International Journal of Rock Mechanics and Mining Sciences & Geomechanics Abstracts. 28, 5(1991), pp. 144-159.

[2] Ilamparuthi, K.; Dickin, E. A. Predictions of the uplift response of model belled piles in geogrid-cell-reinforced sand. // Geotextiles and Geomembranes. 19, 2(2001), pp. 89-109.

[3] Seo, H.; Prezzi, M. Analytical Solutions for a Vertically Loaded Pile in Multilayered Soil. // Geomechnics and Geoengineering. 2, 1(2007), pp. 51-60.

[4] Lee, S. L.; Kog, Y. C.; Karunaratne, G. P. Axially loaded piles in layered soil. // Journal of Geotechnical Engineering, ASCE. 113, 4(1987), pp. 366-381.

[5] Chin, J. T.; Chow, Y. K.; Poulos, H. G. Numerical Analysis of Axially Loaded Vertical Piles and Pile Groups. // Computers & Geotechnics. 9, 9(1990), pp. 273-290.

[6] Poulos, H. G.; Davis, E. H. Pile Foundation Analysis and Design, John Wiley and Sons, New York, 1980.
[7] Guo, W. D.; Randolph, M. F. An efficient approach for settlement of piles groups. // Geotechnique. 49, 2(1999), pp. 161-179.
[8] W. D.Guo. Vertically loaded single piles in Gibson soil. // Journal of Geotechnical and Geoenvironmental Engineering. 126, 2(2000), pp.189-193.
[9] Guo, W. D.; Randolph, M. F. Vertically loaded piles in non-homogeneous media. // International Journal for Numerical and Analytical Methods in Geomechanics. 21, 8(1997), pp. 507-532.
[10] Jiang, J.; Huang, M. S.; Liang, F. Y. Nonlinear simplified analysis of interaction of pile raft foundation. // Journal of Geotechnical Engineering. 30, 1(2008), pp. 112-117.
[11] Motto, E. Approximate elastic-plastic solution for axially loaded piles. // Journal of Geotechnical Engineering. 120, 9(1994), pp. 1616-1624.
[12] Chen, S. P. Research on working behavior and deformation analysis of pile foundation under vertical load. PhD dissertation (2014), Shanghai University, China.
[13] Industry Standard of the People's Republic of China. Code for design of building foundation (GB50007-2011), China Architecture & Building Press, Beijing, 2011.
[14] Qingshan, Li; Shicang, Song. Numerical method, Zhengzhou University Press, Zhengzhou, 2007.
[15] Tiemeng, Wang. Engineering structure crack control, China Architecture & Building Press, Beijing, 1997.
[16] Industry Standard of the People's Republic of China. Technical Code for Building Pile Foundations (JGJ94-2008), China Architecture & Building Press, Beijing, 2008.
[17] Randolph, M. F.; Wroth, C. P. Analysis of deformation of vertically loaded piles. // Journal of the Geotechnical Engineering Division, ASCE. 104, 12(1978), pp. 1465-1488.
[18] Shanghai Xian Dai Architectural Design (Group) Co., Ltd. Research and application on uplift belled cast-in-place pile in Shanghai soft soil area. Research report (2005), Shanghai, Research and Development Center on Basic Sciences of Shanghai Soft Soil Foundation.

Authors' addresses

W. J. Yao, Prof. Ph.D.
Shanghai University
Department of Civil Engineering
149 Yanchang Road, ZhaBei District
200072 Shanghai, P. R. China
E-mail: wenjuan@mail.shu.edu.cn

S. P. Chen, Ph.D.
Shanghai University
Department of Civil Engineering
149 Yanchang Road, ZhaBei District
200072 Shanghai, P. R. China
E-mail: shangping_chen@shu.edu.cn